

Nonlinearity Mechanism and Correction of Sapphire Fiber Temperature Sensor on Blackbody Cavity

Tiejun Cao

School of Electrical & Information Engineering, Hunan International Economics University,
Changsha, 410205, China
Tel.: 86-0731-88760386
E-mail: matlab_wjf@126.com

Received: 23 March 2014 /Accepted: 30 May 2014 /Published: 30 June 2014

Abstract: Based on the principle of blackbody radiation, sapphire optic fiber temperature sensor has been more widely used in recent years, and its temperature range is between 800 ~ 2000 °C, and the response time is in 10^{-2} magnitude, and transient temperature measurement can be high precision in harsh environments. Nonlinear constraints on sapphire fiber temperature sensor affect the accuracy and stability of the sensor. In order to solve the nonlinear problems which exist in the measurement, at first, the sapphire fiber optic temperature sensor temperature measurement principle and nonlinear generation mechanism are studied; secondly piecewise linear interpolation and spline interpolation linearization algorithm is designed with combining the nonlinear characteristics of sapphire optical fiber temperature sensor, and the program is designed on its linear and associated signal processing. Experimental results show that a good linearization of sapphire fiber optic temperature sensor can be achieved in this method. *Copyright © 2014 IFSA Publishing, S. L.*

Keywords: Signal processing, Linearization, Interpolation algorithm, Spline, Sapphire fiber.

1. Introduction

In recent years, sapphire optic fiber temperature sensors are used to measure the temperature of the furnace in metallurgy, refining ore, partly to replace the traditional method of measuring temperature on platinum and rhodium thermocouple [1, 2]. Sapphire optic fiber temperature sensors can be non-contact measurement, and is not affected by electromagnetic interference with small size, light weight, and high sensitivity. However, because the impact of blackbody radiation emission rate and other factors, the nonlinear optical fiber temperature sensor error is relatively large. Therefore, nonlinear calibration is made for optic fiber temperature sensor. Operating principle of sapphire fiber optical fiber

temperature sensor is that sapphire fiber pyrometer is based on the blackbody radiation theory, the probe tip is high temperature sapphire fiber which is produced in a closed blackbody cavity. When the blackbody chamber is placed in the test furnace, the blackbody radiation signal will be issued with a certain function of temperature, so the signal can be sent to photodetector through the fiber, and the output signals are measured, and the tested temperature can be calculated. Microprocessor can be 89C51, after calibration temperature, the piecewise linear approximation is commonly used by software between intermediate interpolation points, nonlinear compensation is generally applied in a logarithmic amplifier, and a temperature sensor head is used as sapphire single crystal optical fiber in sapphire fiber

optic temperature sensor. The sapphire single crystal (Al_2O_3) physical and chemical properties are stability, good mechanical strength, the nature of the insulation, corrosion resistance, and its translucent is good in $0.3 \sim 4.0 \mu\text{m}$ band, the melting point is up to $2046 \text{ }^\circ\text{C}$, and it is an excellent high-temperature near-infrared optical materials [3-5]. So sapphire crystal fiber and fiber optic temperature sensor has been a focus for researchers. These are the main focus on the study of the high temperature sensing performance, transient, and are rarely involved in linearized problem. Linearized sapphire optic fiber temperature sensor has a higher sensitivity, accuracy and reliability.

2. Sapphire Optic Fiber Temperature Sensor Measurement Principle and Nonlinear Mechanism

A sapphire optic fiber temperature measurement system is shown in Fig. 1. The microprocessor can be 89C51, and nonlinear compensation is to use a logarithmic amplifier circuit. Software piecewise linear fitting is commonly used between intermediate interpolations of calibration temperature points. In sapphire optic fiber pyrometer, signals are sent to the photodetector through the fiber to measure the output signals, that is can be calculated measured temperature [7-9].

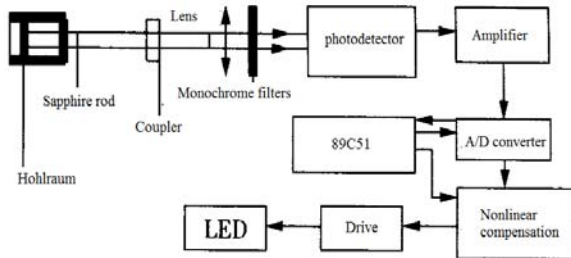


Fig. 1. Sapphire optic fiber temperature measurement system.

Sapphire single optical fiber probe is 1.27 mm in inner diameter of blackbody cavity, the radiated optical signal is transmitted by the total reflection of the inner rod. Sapphire is alumina (Al_2O_3) single crystal, and its melting point is $2050 \text{ }^\circ\text{C}$, and it is a photoconductive material with high mechanical strength, optical transparency, good thermal stability, chemical stability, and it is suitable in high temperature environments [10, 11].

Sapphire optic fiber temperature sensor measurement system is based on the detection of sensor radiation signal, and measured temperature is obtained. According to Planck blackbody radiation law, fiber blackbody cavity temperatures are placed in the T region, and its monochromatic radiation flux [12] is:

$$\varphi(\lambda, T) = \frac{ac_1}{\lambda^5 [\exp(c_2 / \lambda T) - 1]}, \quad (1)$$

where a is the blackbody cavity opening into the fiber area ($a = \pi D^2 / 4 = 5.03 \times 10^{-7} \text{ m}^2$), λ is the wavelength of the radiation, T is the absolute temperature, $c_1 = 3.74183 \times 10^{-16} (\text{W} \cdot \text{m}^2)$ is the first radiation constant, $c_2 = 1.43879 \times 10^{-2} (\text{m} \cdot \text{K})$ is the second radiation constant. The relationship can be represented visually as in Fig. 1 between monochromatic radiation flux $\varphi(\lambda, T)$, a wavelength λ , and the temperature T . Obviously, when the wavelength λ is determined, the monochromatic radiation flux $\varphi(\lambda, T)$ is monotonically increments with the temperature T .

Let measurement system interference filter spectral response function $f(\lambda)$ [13, 14], the spectral response function of a photodetector (PIN tube) is $D(\lambda)$, a monochrome sensor head set emissivity is $\varepsilon(\lambda)$ in taking into account the more general case, the center wavelength of the interference filter is λ_0 , bandwidth $\Delta\lambda$, After radiation optical signal passing the photodetector through the optical fiber, output voltage is:

$$V(\lambda_0, T) = K \int_{\lambda_0 - \Delta\lambda/2}^{\lambda_0 + \Delta\lambda/2} \varphi(\lambda, T) d\lambda = KR(T), \quad (2)$$

$$V(\lambda_0, T) = K \int_{\lambda_0 - \Delta\lambda/2}^{\lambda_0 + \Delta\lambda/2} \varphi(\lambda, T) d\lambda = KR(T), \quad (3)$$

where $\eta(\lambda)$ reflects fiber (including sapphire, crystal fiber, tapered fiber and optical fiber transmission) transmission loss in the optical signal transmission, radiation loss which is caused by insertion loss in optical fiber connector and other optical elements. When the interference filter bandwidth is narrow, it may be assumed:

$$\eta(\lambda) = \eta(\lambda_0), f(\lambda) = f(\lambda_0), D(\lambda) = D(\lambda_0), \quad (4)$$

And substituting into (2) yields, the photodetector output voltage:

$$V(\lambda_0, T) = K \int_{\lambda_0 - \Delta\lambda/2}^{\lambda_0 + \Delta\lambda/2} \varphi(\lambda, T) d\lambda = KR(T), \quad (5)$$

wherein the center wavelength of the interference filter takes $\lambda_0 = 830 \text{ nm}$, the bandwidth $\Delta\lambda = 10 \text{ nm}$, temperature systems is a relationship between temperature and voltage in sapphire fiber blackbody cavity pyrometer, it must know what the value of the coefficient K . K is the coefficient depending on the test device and is a device constant independent of temperature, just to be calibrated at one temperature ($K = 11$). Shown in Fig. 2, it is clearly than the function $U(T)$ and nonlinear relationship with the independent variables T , and the measuring system nonlinearity is a key part, which is the central issue to be addressed in this article [15].

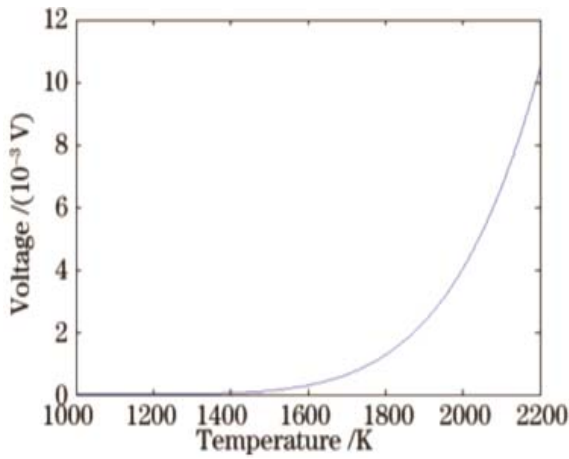


Fig. 2. Relationship between voltage and temperature.

3. Nonlinear Error Sources and Nonlinear Principle

3.1. Nonlinear Error Sources

1) Impact of pre-blackbody cavity emissivity.

Blackbody cavity emissivity $\mathcal{E}(\lambda)$ is determined by parameters such as cavity shape and material. There are two kinds of methods: non-contact measurement, the probe is placed directly in the molten steel. By experimental calibration, $\mathcal{E}(\lambda)$ is little effect on the nonlinear error. However, the non-contact measurement, since the molten metal is not an ideal black body, the $\mathcal{E}(\lambda)$ uncertainty is the main source of nonlinearity errors. Not only to consider the emissivity of the blackbody cavity, but also consider the emissivity of steel and other factors, $\mathcal{E}(\lambda)$ is no longer constant at this time, and it changes with temperature.

2) Effect of nonlinear relationship between the brightness of the black body radiation and the absolute temperature.

It can be seen from the blackbody radiation formula that the radiation intensity is the exponential relationship with the blackbody temperature, so the logarithmic amplifier can be considered to compensate for the measurement.

3) Zero drift affect on photodetector.

In general, silicon photocell or silicon photodiodes are used in photovoltaic, but their common problem is the presence of a temperature drift and zero drift. Therefore the appropriate compensation circuit is needed.

4) Effect of ambient temperature.

Since the furnace temperature is generally not stable, and the measuring sensor system is affected by changes in ambient temperature, a temperature drift is made and therefore because of the photodetector and amplification, a compensation circuit is generally placed in the constant temperature means.

5) Effects of background noise and high frequency interference.

In the environments of the larger electromagnetic interference, the impact of the background noise and high frequency interference are considered in measurements, such as measuring the induction furnace temperature. Although the fiber itself is not affected by electromagnetic interference, but the behind measuring circuit may be disturbed. Therefore the appropriate parameter low-pass filter should be selected to remove interference and improve the stability of the instrument before the measurement.

3.2. Nonlinear Principle

Fig. 3 shows a schematic diagram of the nonlinear calibration sensor.

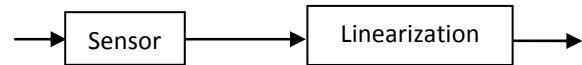


Fig. 3. Correction schematics.

In figure, an input of sensor is variable x , the sensor output variable y , and $y = f(x)$. Sensor output y is the linear input unit, a linear output unit c , and $c = g(y)$. Input-output relationship is nonlinear functional relationship.

$$y = f(x) \quad (6)$$

$$c = g(y) \quad (7)$$

From (7) we can

$$x = f^{-1}(y) \quad (8)$$

After the series linearization, a hope that the input and output of the entire system should be a linear relationship

$$c = sx = sf^{-1}(y) \quad (9)$$

4. Linearization Techniques

4.1. Piecewise Linear Interpolation

Given a division of interval $[a, b]$, $\pi: a = x_0 < x_1 < \dots < x_{n-1} < x_n = b$, $x \in [x_{i-1}, x_i]$

$$f(x) \approx P_i(x) = \frac{x - x_{i-1}}{x_i - x_{i-1}} y_i + \frac{x - x_i}{x_{i-1} - x_i} y_{i-1} \quad (10)$$

where $P_i(x)$ is $f(x)$ piecewise linear interpolation function.

Linearization step are:

$$1) \text{ From (5) } V(\lambda_0, T) = K \int_{\lambda_0 - \Delta\lambda/2}^{\lambda_0 + \Delta\lambda/2} \varphi(\lambda, T) d\lambda,$$

calculating the value T in $T = 1000 \sim 2200$ K;

2) Interpolation function is derived from (10), piecewise linear interpolation image is obtained as shown in Fig. 4.

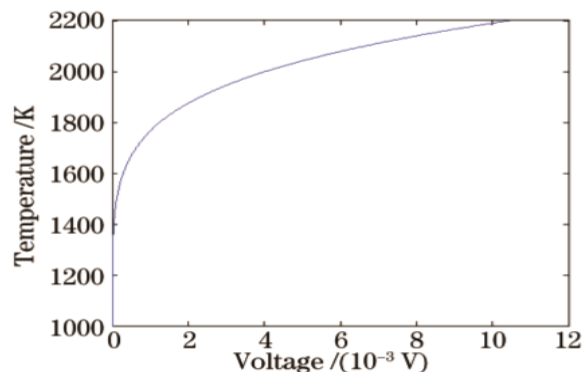


Fig. 4. Piecewise linear interpolation correction function graph.

Piecewise linear interpolation function is easy to implement, but not smooth enough (after amplification), following, the cubic spline interpolation is used to complete linearization in high precision and smooth.

4.2. Cubic Spline Interpolation

Cubic spline interpolation: given interval $[a, b]$ is a division of $\pi: a = x_0 < x_1 < \dots < x_{n-1} < x_n = b$

If $S(x)$ satisfies the condition

$$1) y_i = S(x_i)$$

2) Cubic polynomial on in each sub-interval $[x_{i-1}, x_i]$;

3) $S(x)$ and its derivative until the $(n-1)^{th}$ derivative are continuous in the interval $[a, b]$, $S(x)$ is a cubic spline interpolation function.

$S(x)$ expression on each sub-interval $[x_{i-1}, x_i]$

$$S(x) = S(x_i) = a_i(x-x_i)^3 + b_i(x-x_i)^2 + c_i(x-x_i) + d_i. \quad (11)$$

$$x \in (x_{i-1}, x_i) \quad (i = 1, 2, \dots, n),$$

where a_i, b_i, c_i, d_i is the pending constant. Interpolation conditions:

$$S(x_i) = f(x_i), \quad (i = 1, 2, \dots, n) \quad (12)$$

The continuous and smooth conditions of the $(n-1)$ node is:

$$\left. \begin{aligned} S(x_i - 0) &= S(x_i + 0) \\ S'(x_i - 0) &= S'(x_i + 0) \\ S''(x_i - 0) &= S''(x_i + 0) \end{aligned} \right\} \quad (i = 1, 2, \dots, n-1) \quad (13)$$

From (12), (13) two type plus $S(x_0) = y(x_0)$ boundary conditions can be uniquely identified $S(x)$. Take steps to complete a linear interpolation.

Linearization step are:

1) From (5)

$$V(\lambda_0, T) = K \int_{\lambda_0 - \Delta\lambda/2}^{\lambda_0 + \Delta\lambda/2} \varphi(\lambda, T) d\lambda$$

Calculating $T = 1000 \sim 2200$ K corresponding to the value V ;

2) Taking $T_0 = 1000$ K, $T_n = 2200$ K, calculating $V(T_0), V(T_n)$;

3) Derivative formula is demanded to derive the value of $T(V_0), T(V_n)$ by the implicit function;

4) The interpolation function could be obtained by the condition.

The resulting coefficient of spline interpolation function is 1200×4 matrix, here are the first four lines, such as (14) below.

$$(a_i, b_i, c_i, d_i) = 1.0 \times 10^{23} \times \begin{bmatrix} -2.80781245177285, 0.000000000000, 0.000000, 0.0000 \\ 0.83902766727553, -0.0000002032616, 0.00000, 0.00000 \\ -0.11713871281705, -0.00000001413661, 0.00000, 0.0000 \\ 0.12594201812770, -0.00000001501725, 0.000000, 0.00000 \\ \dots \end{bmatrix} \quad (14)$$

The image of resulting function is shown in Fig. 5.

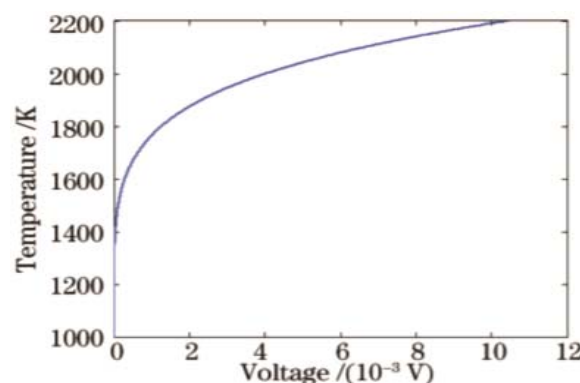


Fig. 5. Cubic spline correction function graph.

5. Error Analysis and Experimental Verification

5.1. Error Analysis

Correction function of piecewise linear interpolation error.

Let $f(x)$ in $[a, b]$, there is second continuous derivative $f''(x)$, then the error estimates for piecewise linear interpolation correction function is:

$$|R(x)| = |f(x) - P1(x)| \leq M h^2 / 8, x \in [a, b], \quad (15)$$

where $|\max f(x)|, h = \max_{1 \leq i \leq n} |x_i - x_{i-1}|$.

From (15), calculating

$$|R(x)| \leq 6.833 \times 10^{-8} \quad (16)$$

Cubic spline interpolation error correction function.

In [a, b], there is four order consecutive derivative $f^{(4)}(x)$, the error estimates for the cubic spline interpolation correction function is:

$$\|f^{(m)} - S^{(m)}\| \leq c_k h^{k-m} \|f^{(4)}\|, (m = 0, 1, 2), \quad (17)$$

where

$$\max_{1 \leq i \leq n} |x_i - x_{i-1}|, c_0 = 1/16, c_1 = c_2 = 1/2.$$

From (17), we obtain

$$|f(x) - S(x)| \leq \frac{1}{16} h^4 \|f^{(4)}\|, \quad (18)$$

From (18), we obtain

$$|f(x) - S(x)| \leq 4.519 \times 10^{-5} \quad (19)$$

From (16), (19), error is very small in linear method, there is a very good accuracy.

5.2. The Experimental Results

Input - output curve fitting is shown in Fig. 6 at a given constant temperature 1200 K, 1238 K, 1369 K, 1479 K, 1568 K, 1896 K and 2013 K for linearization device.

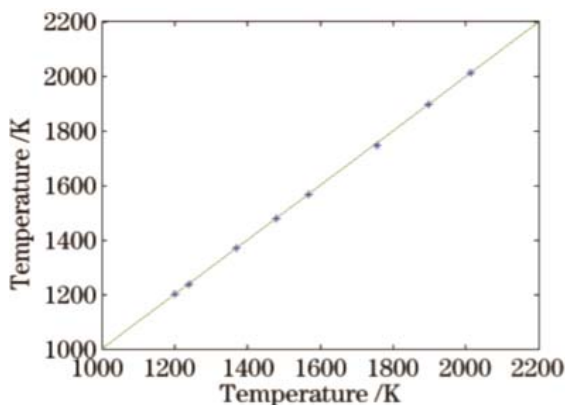


Fig. 6. Calibration curve fitting results.

6. Conclusions and Outlook

According to experimental results: nonlinearity correction signal is achieved in the sapphire optic fiber temperature sensor by the linear algorithm of piecewise linear interpolation and cubic spline interpolation. The error of linearization device is far less than 1 °C. This method is a practical, feasible soft linear method. Linearized temperature is range of 800 ~ 2000 °C in the sapphire fiber measuring temperature system, and the response time is 20 ms with a resolution of 1 °C. These can effectively improve the measurement accuracy of the system, and improve the stability of the sensor.

References

- [1]. Shen Yonghang, Sapphire Fiber Thermometer Ranging from the Room Temperature to 1800 °C, *Acta Optica Sinica*, 20, 1, 2000, pp. 41-45.
- [2]. Xia Jie, Hu Hai-Hua, He Jing-Lei, Shen Yong-Hang, Passively Q-Switched Laser Operation of Composite Cr4+: YAG-Nd3+: YAG Crystal Fiber, *Chinese Journal of Lasers*, 32, 6, 2005, pp. 92-96.
- [3]. Zhang Yue-Fang, Ye Lin-Hua, Qiu Yan-Qing, Study on Optical Properties of Sapphire Fiber under High Temperature, *Semiconductor Optoelectronics*, 30, 5, 2009.
- [4]. Yan Tao, Zhao Jing, Yuan Yu-Hua, Wang Zhi-Hao, Study on the calibration and test system of ultrahigh sapphire-fiber temperature sensor, *Electronic Design Engineering*, 21, 9, 2013, pp. 53-57.
- [5]. Wang Shu-Tao, Che Ren-Sheng, Wang Yu-Tian, etc., Sapphire fiber thermal probe based on wavelet transform, *Journal of Applied Optics*, 27, 5, 2006, pp. 786-789.
- [6]. Wang Gao, Xu Zhao-Yong, Zhou Han-Chang, Transient High Temperature Measurement Based on Sapphire Fiber Sensor and Calibration Technology, *Journal of Optoelectronics Laser*, 16, 4, 2005, pp. 88-91.
- [7]. Hao Xiao-Jian, Li Kejie, Liu Jian, Zhou Han-Chang, Research on characteristic parameter of sapphire fiber blackbody cavity transient high temperature sensor measurement system, *Chinese Journal of Scientific Instrument*, 29, 10, 2008, pp. 68-73.
- [8]. Gui Yi, Hao Xiao-Jian, Zhou Han-Chang, Calibration system of sapphire-fiber temperature sensor, *Transducer and Microsystem Technologies*, 2008, 27, 8, pp. 15-18.
- [9]. Ji Yu-Ling, Xu Peng, The high nonlinear photonic crystal fiber, *Laser Journal*, 5, 2013, pp. 24-28.
- [10]. S. M. Abdur Razzak, Yoshinori Namihira, Numerical design of high nonlinear coefficient of microstructure optical fibers, *Optik*, 122, 2011, pp. 1084-1087.
- [11]. T. L. Wu, C. H. Chao, A novel ultraflattened dispersion photonic crystal fiber, *IEEE Photonics Technology Letters*, 2005, pp. 67-69.
- [12]. Wang Yan-Lei, Luan Mei-Sheng, Yu Tong-Yan, Calibration of high-temperature flame measurement device, *Infrared Technology*, 07, 2009, pp. 399-402.
- [13]. Yonghang Shen, Shuying Chen, Weizhong Zhao, Growth characteristics and potential applications in optical sensors of composite Cr4+:yttrium-aluminum-garnet (YAG)-Nd3+:YAG crystal fiber,

- Review of Scientific Instruments*, 03, 2003, pp. 1187-1191.
- [14]. Yonghang Shen, Shuying Chen, Weizhong Zhao, Composite Cr⁴⁺:YAG-Nd³⁺:YAG crystal fiber: growth characteristics and passively Q-switched laser operation, *SPIE*, 2002, pp. 20-27.
- [15]. Ye L. H., Shen Y. H., Zhaow Z. H., Sapphire fiber thermometers based on fluorescence lifetime measurement, *Journal of Optoelectronics Lasers*, 01, 2002, pp. 83-87.

2014 Copyright ©, International Frequency Sensor Association (IFSA) Publishing, S. L. All rights reserved.
(<http://www.sensorsportal.com>)



CALL FOR PAPERS

IEEE SENSORS 2014 is intended to provide a forum for research scientists, engineers, and practitioners throughout the world to present their latest research findings, ideas, and applications in the area of sensors and sensing technology. IEEE SENSORS 2014 will include keynote addresses and invited presentations by eminent scientists. The Conference solicits original state-of-the-art contributions as well as review papers.

Topics of interest include but are not limited to:

Phenomena, Modeling, and Evaluation
Chemical and Gas Sensors
Biosensors
Optical Sensors
Mechanical and Physical Sensors
Sensor/Actuator Systems
Sensor Networks
Other Sensor Topics
- Materials, processes, circuits, signals and interfaces, etc.

Publication Plans

Presented papers will be included in the Proceedings of IEEE SENSORS 2014 and in IEEE Xplore. Authors may submit extended versions of their paper to the IEEE Sensors Journal.

Exhibition & Partnership Opportunities

The Conference exhibit area will provide your company or organization with the opportunity to inform and display your latest products, services, equipment, books, journals, and publications to attendees from around the world.

For further information, contact:

Lauren Pasquarelli
Conference Catalysts, LLC
Phone: +1 352 872 5544
lauren@conferencecatalysts.com

Conference Officials

General Co-Chairs
Cándid Reig - University of Valencia, Spain
Lina Sarro - TUDelft, The Netherlands
Technical Program Chair
Ignacio R. Matías - Public University of Navarra, Spain
Tutorial Chair
Arnaldo D'Amico - URome, Italy
Special Sessions Chair
Alexander Fish - Bar-Ilan University, Israel
Publicity Chair
Edward Grant - North Carolina State University, USA
Liasion with Industry and Administration Chair
Javier Calpe - Analog Devices, Spain
Local Chair
Jaime Lloret - Polytechnic University of Valencia, Spain
Treasurer
Mike McShane - Texas A&M University, USA

Important Dates

Special Session Proposal deadline: March 28, 2014
Tutorial Proposal Submission Deadline: March 28, 2014
Abstract Submission Deadline: April 11, 2014
Author Notification: June 20, 2014
Final Full Paper Submission (4 Pages): July 25, 2014
Presenting Author and Early-Bird Registration Deadline: July 25, 2014
All submissions shall be checked by means of [CrossCheck](#) to prevent plagiarism.

Conference web site: ieeesensors2014.org

